applied sciences

MDPI

Article

Accumulation of Methylmercury in the High-Altitude Lake Uru Uru (3686 m a.s.l, Bolivia) Controlled by Sediment Efflux and Photodegradation

Stéphane Guédron [1,2,*], Dario Achá [3,*], Sylvain Bouchet [4], David Point [3,5], Emmanuel Tessier [4], Carlos Heredia [3], Stéfany Rocha-Lupa [3], Pablo Fernandez-Saavedra [3], Marizol Flores [2,5], Sarah Bureau [1], Israel Quino-Lima [2] and David Amouroux [4,*]

1 Univ. Grenoble Alpes, Univ. Savoie Mont Blanc, CNRS, IRD, IFSTTAR, ISTerre, 38000 Grenoble, France; sarah.bureau@univ-grenoble-alpes.fr
2 Laboratorio de Hidroquímica—Instituto de Investigaciones Químicas—Universidad Mayor de San Andrés, Campus Universitario de Cota-Cota, casilla, 3161 La Paz, Bolivia; marizol_775@hotmail.com (M.F.); israelquino@hotmail.com (I.Q.-L.)
3 Unidad de Calidad Ambiental (UCA)—Instituto de Ecología—Universidad Mayor de San Andrés, Campus Universitario de Cota Cota, casilla, 3161 La Paz, Bolivia; david.point@ird.fr (D.P.); cr_heredia_a@hotmail.com (C.H.); bio_fany@hotmail.com (S.R.-L.); pablo86fernandez@hotmail.com (P.F.-S.)
4 Univ. de Pau et des Pays de l'Adour, E2S UPPA, CNRS, IPREM, Institut des Sciences Analytiques et de Physico-chimie pour l'Environnement et les Matériaux, Pau, France; sylvain.bouchet@eawag.ch (S.B.); emmanuel.tessier@univ-pau.fr (E.T.)
5 Géosciences Environnement Toulouse, UMR5563—IRD UR 234, Université Paul Sabatier, 14 Avenue Edouard Belin, 31400 Toulouse, France
* Correspondence: stephane.guedron@ird.fr (S.G.); darioAchá@yahoo.ca (D.A.); david.amouroux@univ-pau.fr (D.A.); Tel.: +33-476-63-59-28 (S.G.)

Received: 14 October 2020; Accepted: 4 November 2020; Published: 9 November 2020

Abstract: In shallow aquatic environments, sediment is a significant source of monomethylmercury (MMHg) for surface water (SW). High-altitude aquatic ecosystems are characterized by extreme hydro-climatic constraints (e.g., low oxygen and high UV radiation). We studied, during two seasons, the diel cycles of MMHg in SW and sediment porewaters (PW) of Lake Uru Uru (3686 m a.s.l, Bolivia) contaminated by urban and mining activities. Our results show that diel changes in SW MMHg concentrations (up to 1.8 ng L^{-1}) overwhelm seasonal ones, with higher MMHg accumulation during the night-time and the dry season. The calculation of MMHg diffusive fluxes demonstrates that the sediment compartment was the primary source of MMHg to the SW. Most MMHg efflux occurred during the dry season (35.7 ± 17.4 ng m^{-2} day^{-1}), when the lake was relatively shallow, more eutrophicated, and with the redoxcline located above the sediment–water interface (SWI). Changes in MMHg accumulation in the PWs were attributed to diel redox oscillations around the SWI driving both the bacterial sulfate reduction and bio-methylation. Finally, we highlight that although MMHg loading from the PW to the SW is large, MMHg photodegradation and demethylation by microorganisms control the net MMHg accumulation in the water column.

Keywords: monomethylmercury; water–sediment interface; diel and seasonal cycles; photodegradation

1. Introduction

Lake sediment is known to be an important source of mercury (Hg) species, including the neurotoxic monomethylmercury (MMHg) for overlying waters [1], through their diffusion and advection under dissolved and colloidal phases [2–6]. Hg methylation mainly occurs in sub to anoxic surficial sediments

or biofilms developed at the sediment–water interface (SWI), implying various microorganisms such as methanogens, sulfate-reducing (SRB), and iron-reducing (IRB) bacteria [7–10]. In shallow environments (e.g., shallow lakes, lagoons, ponds), both the shear stress and the bio-irrigation driven by tides, wind, and benthic organisms enhance the upward release of elements contained in the sediment porewater towards the water column [2–6,11–13]. Such MMHg exchange is mainly regulated by the position of the redox front around the SWI where it is mainly produced, the sediment structure (e.g., porosity, tortuosity), and the abundance and type of (in)organic ligands [14,15] and colloids [16].

In high-altitude shallow lakes, extreme hydro-climatic constraints (e.g., high UV radiation and low oxygen) result in large diel variations of the water column's biogeochemical and physical parameters that can overwhelm seasonal amplitude [17]. This is the case in Lake Uru Uru (3686 m above sea level (a.s.l.)), one of the most Hg-contaminated lakes of the Bolivian Altiplano [18,19]. Previous studies [18,19] have shown that urban and mining discharges to the lake, combined with the strong diurnal biogeochemical gradients, have resulted in large diel variability in MMHg levels (0.2 to 4.5 ng L^{-1}) in the water column. The quantification of methylation potential during incubation experiments with enriched isotopes has suggested that sediments could be the major source of MMHg for the water column [18]. Nevertheless, the sediment–water exchange has not yet been assessed.

In this work, we studied Hg and MMHg sediment–water column exchanges in Lake Uru Uru during two 36-h cycles performed at the end of the wet (May) and at the end of the dry (November) seasons of 2014. Hg speciation was measured in the water column (i.e., filtered, particulate, and dissolved gaseous Hg) and in the surficial sediment porewater. We also calculated Hg and MMHg diffusive fluxes at the SWI to assess the sediment contribution in MMHg effluxes toward the water column. The final objective was to identify the biogeochemical and physicochemical factors influencing these sediment–water exchanges and to evaluate those regulating the accumulation of MMHg in the water column.

2. Materials and Methods

2.1. Lake Uru Uru General Settings

Lake Uru Uru (3686 m a.s.l.) is located in the central part of the Bolivian Altiplano region (Figure 1), south of Oruro city. This shallow aquatic ecosystem is a human-made reservoir mainly supplied by the Rio Desaguadero waters. Depending on the season, the lake surface and depth vary between 120 and 350 km^2 and from 0.25 to 1 m, respectively, representing a change in lake volume up to 12 times between the two seasons.

Historical and current mining (e.g., Au, Ag, and Sn) and smelting activities in the region have led to the contamination of the lake by various metals, including Hg [19,20]. In addition, the recent urban development has resulted in the almost permanent eutrophication of this shallow aquatic ecosystem [21]. A sharp contrast exists between the northern and southern parts of the lake, with a higher density of sedge (*Schoenoplectus totora*), grass (*Ruppia* spp.), and algae (Characeae) in the southern part [22]. Previous investigations demonstrated that the diel variability (e.g., temperature, oxygen) in the lake could overwhelm seasonal variations [18]. Furthermore, the synergistic effect of mining (i.e., acid mine drainage (AMD)) and urban effluents from both the Oruro and Huanuni areas (Figure 1) to this shallow lake were proven to enhance Hg methylation, with the sediment being the main source of MMHg during the dry season [19].

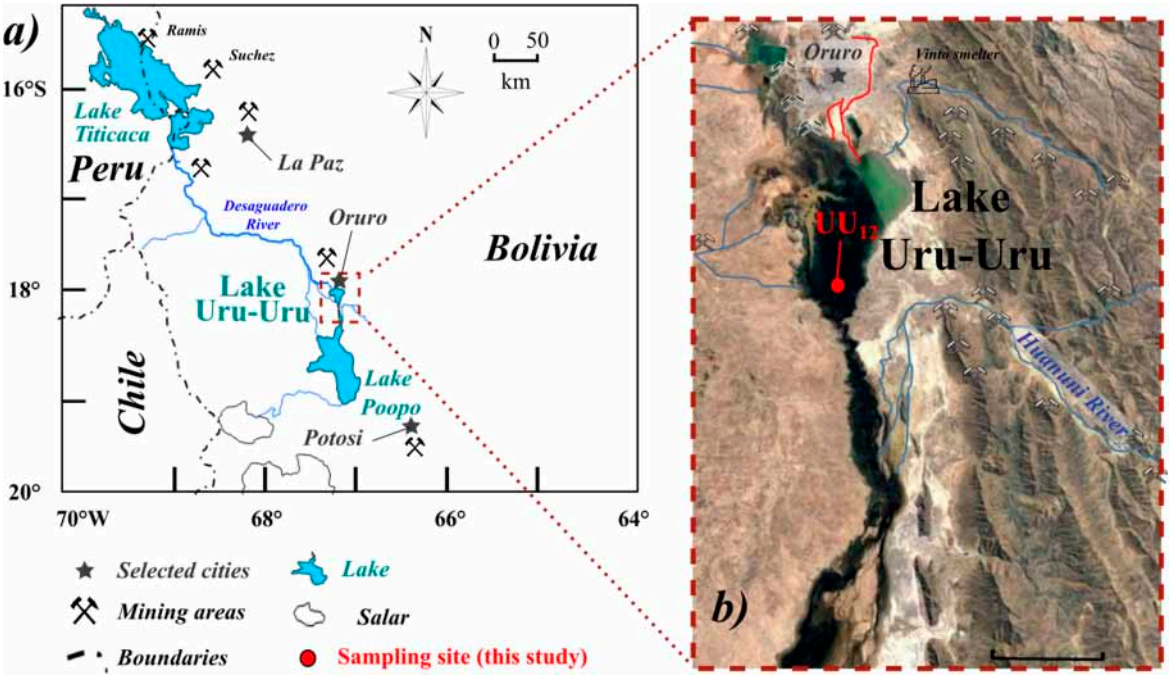

Figure 1. (**a**) Study site location: location of Lake Uru Uru in the Bolivian Altiplano and (**b**) sampling site (UU_{12}) in the southern part of the lake.

2.2. Sampling Location, Strategy, and Elemental Analysis

Surface water and sediment porewater samples were collected during two campaigns performed in May (end of the wet season) and November (end of the dry season) 2014. Surface water was sampled with a Teflon-coated Go-Flo trace metals sampler. Samples were then stored unfiltered or filtered (0.22 µm PVDF) in acid-washed FEP Teflon containers and acidified (except for dissolved gaseous mercury samples) with HCl (0.5%, *v*/*v*, Ultrex grade—Baker). Surface sediment porewaters (0–5 cm) were sampled with 5 cm long microporous polymer tube samplers (RhizonCSS®, 0.2 µm porosity; Rhizosphere Research Products, the Netherlands) over ~4 h, following published protocols [3,23].

Dissolved gaseous mercury (DGM) was purged from unfiltered water samples on-site within ~0.5 h after sampling and collected on gold-coated sand traps [24]. DGM was analyzed by thermodesorption (600 °C) and cold vapor atomic fluorescence spectrometry (CV-AFS) [24]. Filtered (F) and unfiltered (UNF) total mercury concentrations (THg) in surface and pore waters were determined by cold vapor atomic fluorescence spectrometry (CV-AFS) after conversion of all mercury species into Hg0 followed by detection using a Tekran® (Model 2500, Canada) [25,26]. Filtered monomethylmercury ($MMHg_F$) concentrations were analyzed using an ethylation purge and trap-gas chromatograph-AFS analyzer (MERX System, Brooks Rand®, Seattle, WA, USA) following published protocols [27,28]. All samples were run in duplicate and quantified using the standard addition technique. Unfiltered monomethylmercury ($MMHg_{UNF}$) concentrations were analyzed by propylation ID-GC–ICPMS (S.I.2.2) following published protocols [4,29,30].

Dissolved organic carbon concentrations (DOC) were determined using a Non-Dispersive Infra-Red (NDIR) CO_2 Shimadzu® (Model VCSN, Japan) spectrometer after humid oxidation in a sodium persulfate solution at 100 °C. Major elements (Ca, Si, K, Na, Mg, and S) in filtered water (SW and PW) were measured by ICP-AES (Varian model 720ES) within the analytical chemistry platform of ISTerre (OSUG-France) and trace elements (Fe, Al, Mn, V, Sb) by ICP-MS (Nexion, Perkin Elmer) within the analytical chemistry platform of Univ. de Pau et des Pays de l'Adour (UPPA). Anions were measured by ionic chromatography using a 332 Metrohm apparatus and its accuracy was evaluated with a Carl Roth 2668.1 standard. Hydrogen sulfide (H_2S) was determined using a

modification of the diamine method described elsewhere [31,32] and analyzed with HPLC (Agilent) after calibration with a Radiello® solution (Code 171, Italy) for H_2S [28].

A submersible multiparameter probe (HI-9828, Hanna Instruments, Woonsocket, RI, USA) was used to characterize the water physico-chemistry (pH, conductivity, dissolved oxygen concentration and saturation, and temperature). Data collection was conducted every three seconds for two minutes at the surface (0–10 cm) and above the sediment–water interface (SWI) at each time of sampling [28].

2.3. Sediment–Water Flux Measurement and Calculation

Molecular diffusion from sediment to overlying water was estimated through the calculation of diffusive flux for Hg(II) (= THg − MMHg) and MMHg at the SWI using the measured concentration gradient and Fick's first law [33,34]:

$$Jsed = -Ø/Dsed\ (\partial C/\partial z)$$

where Jsed ($ng.m^{-2}\ d^{-1}$) is the diffusive flux from the sediment, Ø is the porosity (Ø = 0.78 [20]), Dsed is the diffusive coefficient in sediment (2×10^{-6} $cm^2\ s^{-1}$ and 1.2×10^{-5} $cm^2\ s^{-1}$ for Hg(II) and MMHg ionic/molecular diffusion coefficient in water [35]), and $\partial C/\partial z$ is the linear concentration gradient through the SWI. Positive Jsed indicates an upward-directed flux (efflux from the sediment into the overlying water column), and negative Jsed indicates a downward-directed flux (influx from the water column into the sediment).

3. Results

3.1. Diel and Seasonal Variations of Mercury Species in Surface Water

The water column was oxic during both seasons, with the lowest oxygen levels (O_2 = 76 ± $23\%_{saturation}$) and redox potential values [i.e., oxydo-reduction potential (ORP) = −8 to −72 mV] found during the dry season compared to the wet one (O_2 = 93 ± $17\%_{sat}$), where redox (i.e., ORP = 192 to −115 mV) was only negative during the night, resulting from algal respiration and sulfate reduction (H_2S = 51 ± 42 μg L^{-1}, Figure 2a,b).

Dissolved gaseous mercury (DGM = 11.2 ± 9.9 pg L^{-1}) in surface water (SW) was mainly in the form of Hg(0) [19] and was overall low and never exceeded 1% of THg_{UNF} for both seasons (Figure 2a), similar to previous studies in Lake Uru Uru [19] and Lake Titicaca [24] but in the lowest range of values reported for temperate freshwater lakes [36,37]. Higher DGM levels were found during the dry season (21.0 ± 7.5 pg L^{-1}), which were around four times higher than during the wet one (5.6 ± 5.5 pg L^{-1}).

Average unfiltered (UNF) concentrations of THg (3.3 ± 1.0 ng L^{-1}) and MMHg (0.6 ± 0.2 ng L^{-1}) were 3 to 10 times higher than those measured in Lake Titicaca [2,24] reflecting the local mining contamination and high MMHg production in this ecosystem [18,19]. Both the average filtered (F) and unfiltered (UNF) THg and MMHg levels in surface water (Figure 2c,d) were similar between the two seasons. In contrast, filtered alkali and alkaline-earth metal concentrations (e.g., Li, Na, K, Mg, Ca, and Sr) and DOC increased by two to three times during the dry season due to the evaporation and concentration of ions in water (Figure 2b and Figure S1).

The diel variability of F and UNF MMHg concentrations overwhelmed the seasonal one, with the highest values measured during the night-time when oxygen levels dropped (Figure 2a), resulting from the aquatic ecotopes' respiration. MMHg/THg percentages were high in surface waters for both seasons. However, they presented larger diel variations, with lower average values during the dry season (i.e., 35 ± 20% and 26 ± 7% for F and UNF, respectively) compared to the wet one (i.e., 42 ± 4% and 35 ± 6%, Figure 2e).

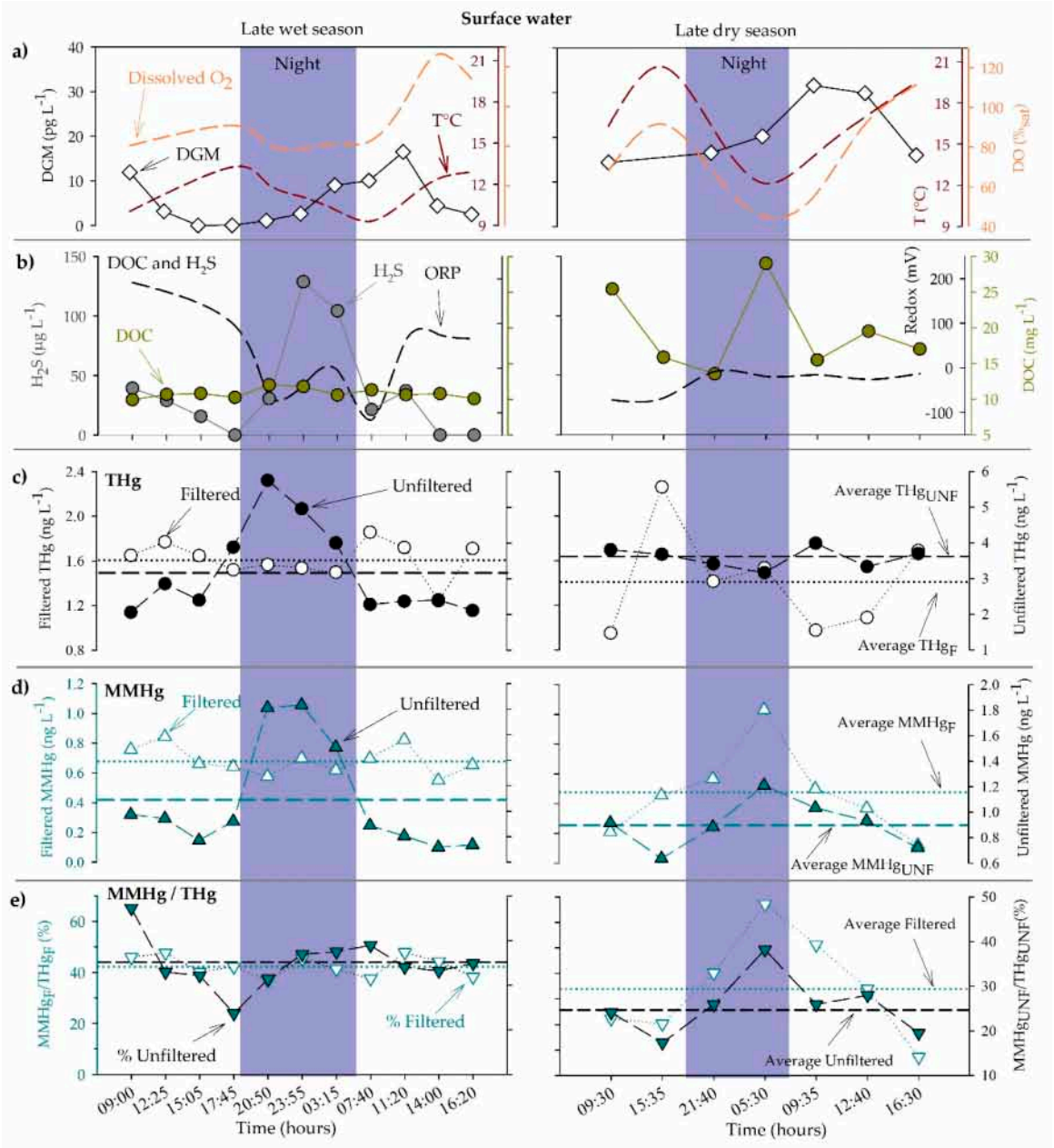

Figure 2. (**a**) Dissolved gaseous Hg (DGM), dissolved oxygen saturation percentage ($\%_{sat}$), and temperature (T °C); (**b**) dissolved organic carbon (DOC), hydrogen sulfide (H_2S), and redox potential (ORP); (**c**) filtered (F, empty symbols) and unfiltered (UNF, black symbols) THg concentrations; (**d**) filtered (F, empty symbols) and unfiltered (UNF, dark cyan symbols) MMHg concentrations; and (**e**) percentage MMHg over the THg concentrations in the F (empty symbols) and UNF (dark cyan symbols) in surface water during the wet (left panels, 20–21 May 2014) and the dry (right panel, 18th to 19th November 2014) seasons. Lines represent average concentrations for F (dotted line) and UNF (dashed line) species and ratios.

3.2. Diel and Seasonal Variations of Mercury Species in Surface Sediment Porewater

Filtered THg (8.8 ± 3.3 ng L^{-1}) and MMHg (1.7 ± 1.1 ng L^{-1}) levels in surface sediment PW (Figure 3a) were 2 to 8 times higher than those of SW. In contrast to SW, large seasonal differences were observed in the PW, with higher MMHg concentrations during the dry season (3.0 ± 1.2 ng L^{-1}) compared to the wet one (1.0 ± 0.4 ng L^{-1}, Figure 3b). Percentage MMHg/THg (Figure 3b) was also

higher during the dry season (28.1 ± 11.0%) compared to the wet one (15.5 ± 8.8%), highlighting a higher accumulation of MMHg in surface sediment PW during the dry season.

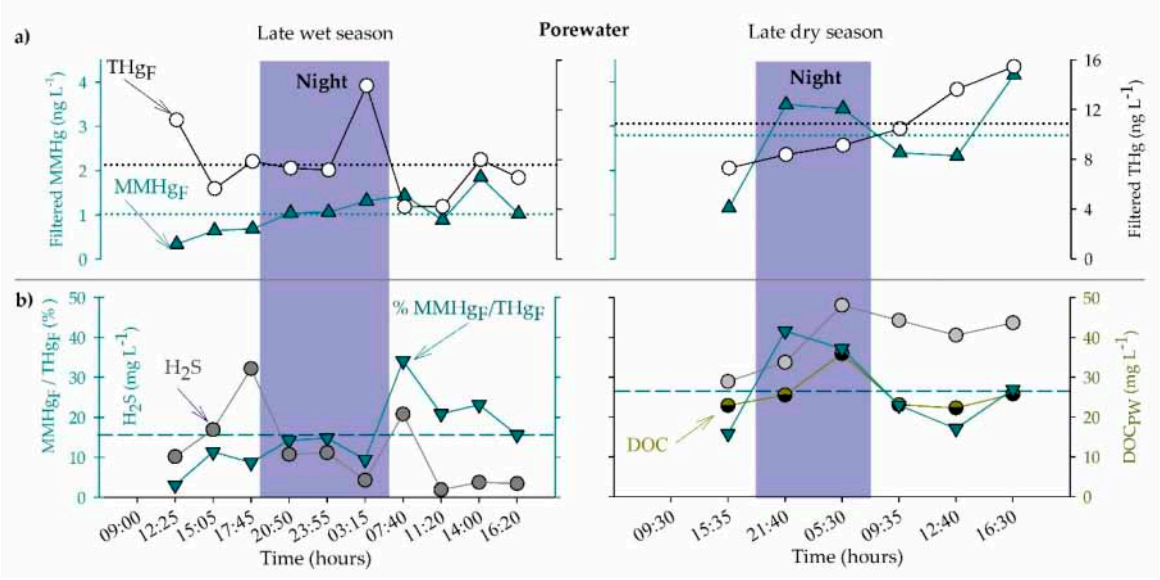

Figure 3. (**a**) Filtered (F) THg (empty circles) and MMHg concentrations (dark cyan triangles up) and (**b**) percentage MMHg over the THg concentrations (dark cyan triangle down), dissolved organic carbon (DOC, semi-filled dark yellow circles), and hydrogen sulfide (H_2S, grey circles) concentrations in sediment porewater during the wet (left panels, 20–21 May 2014) and the dry (right panel, 18th to 19th November 2014) seasons. Lines represent average concentrations for F (dotted line) and MMHg/THg (dashed line) concentrations and ratios.

Diel variations were large for THg, but no specific trend was identified except for a rising trend in concentrations during the day for the dry season. In contrast, MMHg exhibited similar trends as for SW, with rising concentration during the night for the dry season, while they did not vary significantly during the wet season.

DOC concentrations in PWs (26 ± 5 mg L^{-1}, only measured during the dry season) were, on average, 1.5 times higher than those of SW but exhibited a similar diel trend, suggesting that equilibrium was established between these two compartments. Sulfide concentrations were an order of magnitude higher than the one in SW, with at least three times higher average concentrations during the dry season (39.9 ± 7.2 mg L^{-1}) compared to the wet one (12.1 ± 9.0 mg L^{-1}, Figure 3b).

4. Discussions

4.1. DOC and Sulfides Drive MMHg Accumulation in Sediment PW and Effluxes Towards the SW

The high MMHg concentrations found in PW are consistent with a previous study in Lake Uru Uru, which showed evidence that methylation was mediated mostly by SRB in the absence of sunlight [18]. Such nutrient-rich, alkaline waters with elevated levels in DOC and sulfates were also reported to favor the activities of anaerobic bacterial communities [4,23,24,38]. During the wet season, the gradual rise in MMHg concentration in PW during the night illustrates the progressive installation of anoxia in surface sediment PW due to the rising respiration of the aquatic ecotopes, which is also reflected by the drop in dissolved oxygen in overlying waters (Figure 4a). This pattern is exacerbated during the dry season as a result of more eutrophic conditions, which enhance MMHg production and accumulation in the sediments [39]. During this latter season, both DOC and sulfide concentrations were positively correlated ($R = 0.56$, $p < 0.05$), supporting the notion that active sulfate reduction in PW favors DOC release in PWs during the reduction of Fe-oxy(hydr)oxides [40].

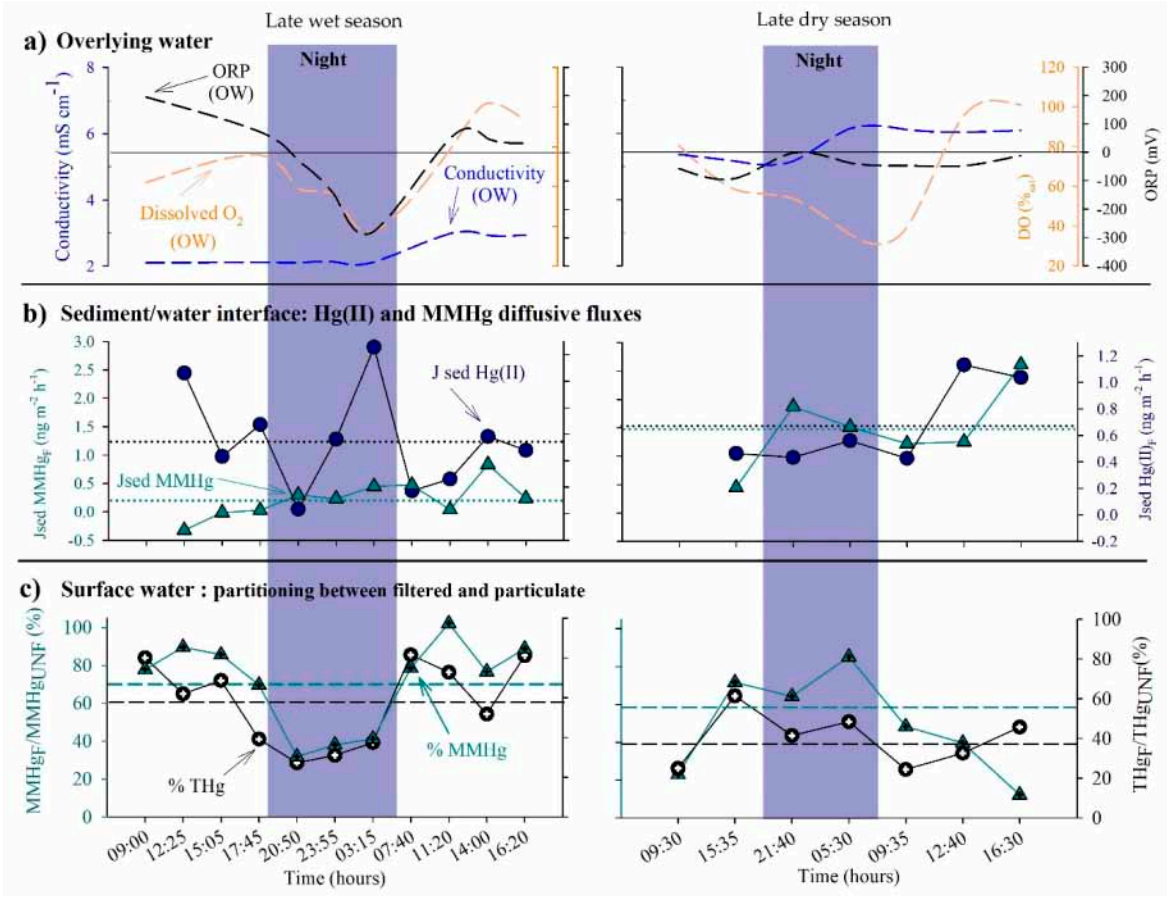

Figure 4. (**a**) Redox potential (ORP), dissolved oxygen saturation percentage (%$_{sat}$), and conductivity in overlying waters (OW) above the sediment–water interface (SWI); (**b**) filtered Hg(II) (=THg − MMHg) and MMHg diffusive fluxes (Jsed) at the SWI and (**c**) partitioning of THg and MMHg between filtered and particulate fractions in surface water, during the wet (left panels) and the dry (right panels) seasons. Lines represent averages for Jsed (dotted line) and for MMHg/THg ratios (dashed line).

Interestingly, positive correlations were also found between sulfide and MMHg concentration ($R = 0.73$, $p < 0.01$, Figure S3) or percentages MMHg/THg ($R = 0.66$, $p < 0.01$), and between percentages MMHg/THg and DOC ($R = 0.66$, $p < 0.01$). This suggests that filtered MMHg was preferentially bound to sulfurized dissolved organic matter (DOM). In addition, the positive correlation found between sulfide and THg concentration (Figure S2) supports a limited precipitation of inorganic Hg with free sulfide or with FeS, which would have restricted the availability of Hg(II) for bio-methylation [41–43]. Hence, this rather supports the presence of Hg-SR complexes, which were reported to increase the bioavailability of Hg(II) for bio-methylation [14,15]. In contrast, sulfide was negatively correlated with chalcophile redox-sensitive elements (i.e., Fe and V, $p < 0.01$, respectively, Figures S2 and S3), supporting the notion that the sulfate reduction in anoxic PWs favors their precipitation as authigenic sulfide minerals.

The calculation of diffusive fluxes (Jsed, Figure 4b) for MMHg and HgII (=THg − MMHg) confirms both the seasonal and diel patterns observed in the PW and SW (Figures 2 and 3). Daily Jsed for HgII (16.2 ± 7.3 ng m^{-2} day^{-1}) and MMHg (35.7 ± 17.4 ng m^{-2} day^{-1}) were higher during the dry season compared to the wet one (13.3 ± 9.1 ng m^{-2} day^{-1} and 5.4 ± 7.8 ng m^{-2} day^{-1} for HgII and MMHg, respectively). These MMHg diffusive fluxes are much lower than those measured in the carbonate-rich sediments of Lake Titicaca (36 to 224 ng m^{-2} day^{-1}) but in the range of those reported for the organic-rich sediment of the same lake (13 to 60 ng m^{-2} day^{-1} [2]) and in coastal environments [3,4,6].

Strikingly, MMHg Jseds were higher than those of HgII during the dry season, whereas the opposite was found for the wet season. This greatly illustrates the major MMHg accumulation in the surface sediment PW and the upward MMHg efflux towards SW during the dry season. In addition, the positive correlation found between sulfide and MMHg Jsed ($R = 0.70$, $p < 0.01$, Figure S3) supports the notion that the upward shift of the redox gradient above the SWI during the dry season has likely favored the diffusion of DOC-bound MMHg or MMHg-SR complexes in the overlying water [14]. In contrast, the lower MMHg Jseds during the wet season likely result from the downward shift of the redox stratification in the epibenthic layers and/or the sediment. Indeed, higher MMHg Jsed during the night-time could be explained by a shallower redox front when the aquatic ecotope respiration dominates and favors upward Hg diffusion [2,44]. In contrast, the macrophytes and algae photosynthesis during the day may favor the water column oxygenation and the scavenging of MMHg in the Fe redox loop and onto submerged macrophytes' periphyton or benthic biofilms and algae [45,46], explaining negative Jsed during the day-time [4,47].

Hence, the stratification within the water column during the dry period likely favored upward MMHg effluxes from the sediment, which was also probably enhanced by the advection of surface PW by wind-induced shear stress in this shallow system as wind was on average 40% higher in November than in May (Figure S4).

4.2. Diel and Seasonal Changes in the Hg Partitioning between Dissolved and Particulate Phases in SW

Previous studies reported limited net Hg methylation potentials in the water column, whereas elevated ones were found in floating bio-organic substrates and surface sediment of Lake Uru Uru [18], supporting elevated MMHg production into fully anoxic environments or surface water microenvironments [12,48,49]. Although average MMHg concentrations were similar between the two seasons, the lower average percentages of filtered and unfiltered MMHg/THg with larger diel variations during the dry season compared to the wet one (i.e., 42 ± 4% and 35 ± 6%) can be explained by changes in water column biogeochemical conditions (i.e., dissolved oxygen, temperature and redox oscillations, and pelagic productivity or mobility), resulting in changes in the partitioning between the suspended solids and the solution. Alternatively, changes in the incident light radiation (see Section 4.3) between the two seasons may explain the seasonal differences.

During the wet season, average percentages of filtered (<0.22 µm) THg and MMHg in surface water were 58 ± 21% and 71 ± 23% of the UNF one, respectively, highlighting that both species were mainly present in the truly dissolved or colloidal phases (Figure 4c). Strikingly, sharp drops in the percentage of F/UNF THg and MMHg fractions (i.e., from ~80 to ~30%, Figure 4c) were found during the night, counterbalanced by the rise in both species onto particles synchronously with the drop in redox to negative values (Figure 2b). These percentages of F/UNF THg and MMHg were found to decrease with rising sulfides ($R = -0.64$ and -0.62, $p < 0.05$, for THg and MMHg, respectively) or DOC concentrations ($R = -0.62$ and -0.55, $p < 0.05$, for THg and MMHg, respectively) supporting the notion that DOC-bound MMHg or MMHg-SR complexes released from surface PW or produced in anoxic niches were sorbed onto suspended inorganic and organic particles. During the onset of reducing conditions, Mn concentrations (Figure S1) rose in the water column as a result of the dissolution of Mn oxides [50], whereas chalcophile redox-sensitive elements (i.e., Fe and V; Figure S1) decreased, likely due to their (co)precipitation as or onto authigenic sulfide minerals [51]. Sulfate concentrations (5.4 ± 5.1 g L^{-1}) were at least an order of magnitude higher than those of Fe, and thus the production of sulfides drives the Fe levels in the SW. Hence, drops in THg_F and $MMHg_F$ levels during reducing conditions found in the night-time period likely resulted from their adsorption or (co)precipitation onto/with colloidal and particulate FeS [2], and onto sulfurized OM [52]. They likely enriched the particulate pool through the flocculation of dissolved OM and the aggregation of colloids when SW became reducing [53,54].

During the dry season, Hg species in the reducing SW showed the opposite trend as for the wet season. THg and MMHg were mostly bound to particles (60 ± 13% and 50 ± 25% for particulate THg

and MMHg, respectively), with higher partitioning onto particles during the day (Figure 4c). Such an opposite trend likely results from the more reducing, oxygen depleted, and sulfide-rich SWs, which favored both the MMHg production, upward efflux from the PW, and its preservation in the truly dissolved or colloidal form during the night in the dry season. In particular, the drop in oxygen was more accentuated during the night in the dry compared to the wet season, possibly resulting from a higher decomposition activity, triggered in turn by a higher productivity during the day. In addition, the higher content of algae and bacteria (both living or dead) in the SW during the dry season could have enhanced Hg and MMHg entrapment during the day as these organisms are known to accumulate MMHg in lake water columns [28,45,46,55]. Indeed, higher radiation levels and SW temperatures have increased biological activities, as illustrated by higher decreases in oxygen saturation (Figure 2a), which could have led to higher active uptake of MMHg by algae during the day [56]. Again, this agrees with reported abundant bio-organic aggregates and/or suspended particles enriched in OM in the water column during the dry season in Lake Uru Uru [18]. Thus, during the nights of the dry season, more MMHg is produced, whereas more uptake and potential demethylation occurs during the day. In addition, algae activity could have facilitated Hg reduction [57], explaining an increase in DGM during the day in the dry season (Figure 2a).

4.3. Solar Radiation Influence on MMHg Photodegradation and DGM Production in Surface Water

Because solar ultraviolet (UV-B) increases by around 10 ± 20% for every 1000 m increase in elevation [58,59], UV radiation intensity at Lake Uru Uru (3686 m a.s.l) is expected to be at least 40 to 80% higher than that measured at sea level [18,60]. The large diurnal and seasonal temperature amplitude gradients between the dry season (12.2 to 20.7 °C) and the wet one (10.0 to 13.3 °C, Figure 2a) broadly reflect these gradients in solar radiation.

For both seasons, filtered and unfiltered MMHg/THg decreased with increasing temperature, with the exception of the filtered phase during the wet season (Figure 5). This trend illustrates the strong influence of UV radiation on MMHg photodegradation [61] at both the diel and seasonal scales, with enhanced degradation of MMHg during the day and the dry season [18]. One cannot exclude higher activation of demethylating bacteria at higher temperatures [62].

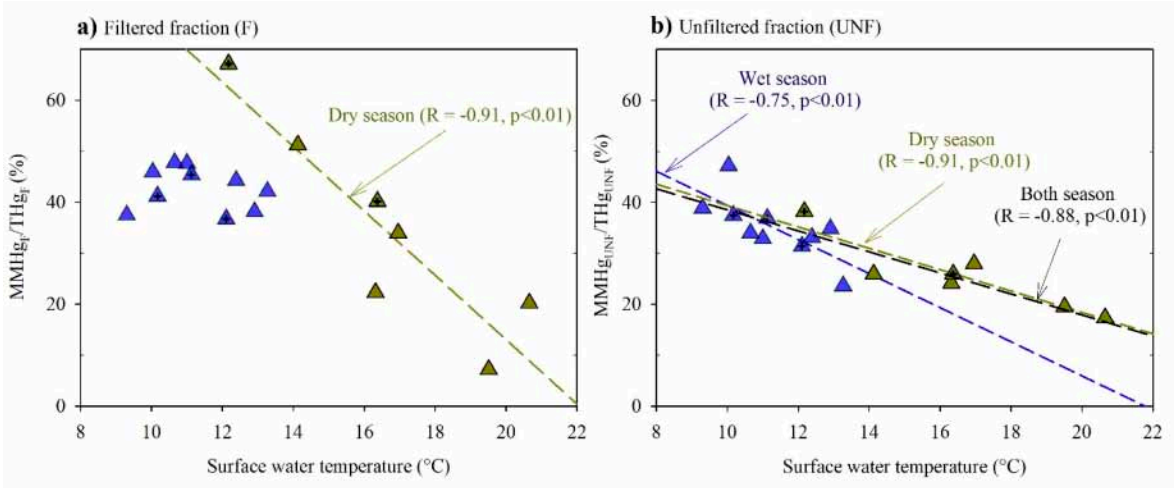

Figure 5. Plots of percentage MMHg/THg in (**a**) the filtered and (**b**) the unfiltered phases vs. surface water temperature. Crossed symbols indicate samples collected during the night-time period.

In addition, a positive correlation was found between DOC concentrations and percentages MMHg/THg ($R = 0.66$, $p < 0.01$) during the dry season, supporting the notion that rising DOC concentrations decreased the efficiency of MMHg photodegradation [63,64]. Although DOC concentration was lower during the wet season, the absence of a relationship between MMHg and SW temperature or DOC for the filtered fraction suggests that photodemethylation was not a primary

sink for MMHg during this season. Indeed, lower insolation, higher water column, possible changes in the composition of photo-reactive DOC species, and/or different MMHg-DOC bindings [65] could have attenuated the radiation effect and reduced MMHg photodegradation efficiency. In particular, higher molecular weight dissolved OM, and a lower abundance of thiol functional groups (RS-) during the wet season compared to the dry one, could have attenuated MMHg photodegradation [66,67]. As mentioned previously, one cannot exclude the possibility of lower biological activity in the wet compared to the dry season, which would also have resulted in lower MMHg biodegradation.

As for MMHg, the overall low DGM (i.e., Hg(0)) concentrations in SW corroborate results from in situ incubations with Hg-enriched isotopes, which reported low biological and photochemical production of DGM in Lake Uru Uru [18]. Although DGM concentrations were low, the higher concentrations found during the dry season likely result from higher solar radiation, higher concentrations of suspended solids, as well as reducing bacteria/algae. Although solar radiations are the main fuel for DGM production during the day, rises in DGM found during the night support the notion of significant bacterial reductions in the dark [57].

5. Conclusions

Our results confirm previous observations made in Lake Uru Uru showing that diel changes in MMHg concentration overwhelm seasonal ones, with higher MMHg accumulation in surface water during the night-time and the dry season. We here bring new insights into the key role of the sediment compartment as a major source of MMHg for the SW, with a larger contribution in MMHg efflux towards the water column during the dry season when the lake is relatively shallow, more eutrophicated, and with the redoxcline likely moving above the SWI. Our results suggest that MMHg accumulation in the PWs fluctuates depending on diel redox oscillations around the SWI, driving both the bacterial sulfate reduction and bio-methylation. We here confirm the previous hypothesis from enriched isotope incubation that MMHg is preferentially produced in the PW and supports its release toward the SW associated with dissolved/colloidal OM or organic thiols. In the water column, both the pelagic light-dependent organisms and the flocculation/aggregation of dissolved OM with colloids drive the MMHg partitioning between dissolved and particulate phases during diel redox oscillations. Finally, although elevated MMHg diffusive fluxes demonstrate that MMHg loading from the porewater to the water column is large, both the photochemical and biological methylmercury degradation control the net MMHg accumulation in the water column.

Supplementary Materials: The following are available online at http://www.mdpi.com/2076-3417/10/21/7936/s1, Figure S1: Seasonal and diel cycles for vanadium (V), manganese (Mn), calcium (Ca); potassium (K), magnesium (Mg), sodium (Na), total sulfur (S), and silicon (Si) in surface water. Figure S2: Scatter plot with linear regression for porewater concentrations of (a) manganese (Mn) vs. hydrogen sulfide (H_2S) and dissolved oxygen (O2—measured in epibenthic water above the SWI with a multiparameter probe); (b) iron (Fe) and vanadium (V) vs. H_2S; (c) Filtered total mercury THg vs. H_2S and V. Linear regression was performed for all data (both seasons). Figure S3: Scatter plot for (upper panels) PW MMHg concentrations vs. hydrogen sulfide (H_2S) and vanadium (V), and (bottom panels) MMHg diffusive fluxes (Jsed MMHg) vs. (H_2S) and redox potential (measured in epibenthic water above the SWI with a multiparameter probe). Figure S4: Average precipitation and wind velocity at Oruro during the period 2010 to 2016 [68].

Author Contributions: Conceptualization, D.A. (David Amouroux), S.G., D.P., D.A. (Dario Achá), and S.B.; methodology, S.G., D.A. (David Amouroux), D.P., S.B., and D.A. (Dario Achá); validation, S.G., D.A. (Dario Achá), D.P., S.B., and D.A. (David Amouroux); methodology, S.G., D.A. (Dario Achá), D.P., S.B., and D.A. (David Amouroux); formal analysis, S.G., D.A. (Dario Achá), S.B., D.P., E.T., S.R.-L., C.H., P.F.-S., M.F., and S.B.; Field investigation, S.G., D.A. (David Amouroux), D.A. (Dario Achá), S.B., D.P., E.T., S.R.-L., C.H., P.F.-S., M.F., I.Q.-L., and S.B.; data curation, S.G.; writing—original draft preparation, S.G.; writing—review and editing, S.G., D.A. (Dario Achá), S.B., and D.A. (David Amouroux); supervision, S.G., D.A. (Dario Achá), S.B., and D.A. (David Amouroux); project administration, D.A. (David Amouroux) and S.G.; funding acquisition, S.G., D.A. (Dario Achá), S.B., and D.A. (David Amouroux). All authors have read and agreed to the published version of the manuscript.

Funding: This research was funded by Agence National pour la Recherche, as a contribution to the LA PACHÁMAMA project (ANR CESA program, No ANR-13-CESA-0015-01, PI: D. Amouroux: david.amouroux@univ-pau.fr), COMIBOL project (INSU CNRS/IRD EC2CO Program, PI: D. Point: david.point@ird.fr), EUTITICACA project (founded by the Impuestos Directos a los Hidrocarburos IDH

administrated by the Universidad Mayor de San Andrés, PI: D. Achá: darioAchá@yahoo.ca) and TRACISOMER supported by a grant from Labex OSUG@2020 (PI: S. Guédron: stephane.guedron@ird.fr). S. Guédron and S. Bureau (ISTerre/IRD/UGA) are part of Labex OSUG@2020 (Investissements d'avenir—ANR10 LABX56).

Acknowledgments: We wish to thank J. Gardon, A. Terrazas, C. González, N. Clavijo, L. Salvatierra, R. Rios, J.C. Salinas, A. Castillo, M. Claure, and Don German Calizaya (Fishermen Association, MAchácamarca, Bolivia) for their help and assistance during the field campaigns.

Conflicts of Interest: The authors declare no conflict of interest.

References

1. Fitzgerald, W.F.; Lamborg, C.H.; Turekian, H.D.; Holland, K.K. 11.4 - Geochemistry of Mercury in the Environment. In *Treatise on Geochemistry*, 2nd ed.; Elsevier: Oxford, UK, 2014; pp. 91–129. [CrossRef]
2. Guédron, S.; Audry, S.; Achá, D.; Bouchet, S.; Point, D.; Condom, T.; Heredia, C.; Campillo, S.; Baya, P.A.; Groleau, A.; et al. Diagenetic production, accumulation and sediment-water exchanges of methylmercury in contrasted sediment facies of Lake Titicaca (Bolivia). *Sci. Total Environ.* **2020**, *723*, 138088. [CrossRef] [PubMed]
3. Guédron, S.; Huguet, L.; Vignati, D.A.L.; Liu, B.; Gimbert, F.; Ferrari, B.J.D.; Zonta, R.; Dominik, J. Tidal cycling of mercury and methylmercury between sediments and water column in the Venice Lagoon (Italy). *Mar. Chem.* **2012**, *130–131*, 1–11.
4. Bouchet, S.; Amouroux, D.; Rodriguez-Gonzalez, P.; Tessier, E.; Monperrus, M.; Thouzeau, G.; Clavier, J.; Amice, E.; Deborde, J.; Bujan, S. MMHg production and export from intertidal sediments to the water column of a tidal lagoon (Arcachon Bay, France). *Biogeochemistry* **2013**, *114*, 341–358.
5. Benoit, J.M.; Shull, D.H.; Harvey, R.M.; Beal, S.A. Effect of bioirrigation on sediment - water exchange of methylmercury in Boston Harbor, Massachusetts. *Environ. Sci. Technol.* **2009**, *43*, 3669–3674. [PubMed]
6. Hammerschmidt, C.R.; Fitzgerald, W.F. Sediment—Water exchange of methylmercury determined from shipboard benthic flux chambers. *Mar. Chem.* **2008**, *109*, 86–97. [CrossRef]
7. Hamelin, S.; Amyot, M.; Barkay, T.; Wang, Y.; Planas, D. Methanogens: Principal methylators of mercury in lake periphyton. *Environ. Sci. Technol.* **2014**, *45*, 7693–7700.
8. Achá, D.; Iniguez, V.; Roulet, M.; Guimarães, J.R.D.; Luna, R.; Alanoca, L.; Sanchez, S. Sulfate-Reducing Bacteria in Floating Macrophyte Rhizospheres from an Amazonian Floodplain Lake in Bolivia and Their Association with Hg Methylation. *Appl. Environ. Microbiol.* **2005**, *71*, 7531–7535. [CrossRef]
9. Garcia Bravo, A.; Bouchet, S.; Guédron, S.; Amouroux, D.; Dominik, J.; Zopfi, J. High methylmercury production under iron-reducing conditions in sediments impacted by sewage treatment plant discharges. *Water Res.* **2015**, *80*, 245–255.
10. Kerin, E.J.; Gilmour, C.C.; Roden, E.; Suzuki, M.T.; Coates, J.D.; Mason, R.P. Mercury methylation by dissimilatory iron-reducing bacteria. *Appl. Environ. Microbiol.* **2006**, *72*, 7919–7921. [CrossRef] [PubMed]
11. Point, D.; Monperrus, M.; Tessier, E.; Amouroux, D.; Chauvaud, L.; Thouzeau, G.; Jean, F.; Amice, E.; Grall, J.; Leynaert, A.; et al. Biological control of trace metal and organometal benthic fluxes in a eutrophic lagoon (Thau Lagoon, Mediterranean Sea, France). *Estuar. Coast. Shelf Sci.* **2007**, *72*, 457–471. [CrossRef]
12. Guédron, S.; Cossa, D.; Grimaldi, M.; Charlet, L. Methylmercury in tailings ponds of Amazonian gold mines (French Guiana): Field observations and an experimental flocculation method for *in situ* remediation. *Appl. Geochem.* **2011**, *26*, 222–229. [CrossRef]
13. Choe, K.Y.; Gill, G.A.; Lehman, R.D.; Han, S.; Heim, W.A.; Coale, K.H. Sediment—Water exchange of total mercury and monomethyl mercury in the San Francisco Bay - Delta. *Limnol. Oceanogr.* **2004**, *49*, 1512–1527. [CrossRef]
14. Skyllberg, U. Competition among thiols and inorganic sulfides and polysulfides for Hg and MeHg in wetland soils and sediments under suboxic conditions: Illumination of controversies and implications for MeHg net production. *J. Geophys. Res. Biogeosci. (2005–2012)* **2008**, *113*, 1–14. [CrossRef]
15. Bouchet, S.; Goni-Urriza, M.; Monperrus, M.; Guyoneaud, R.; Fernandez, P.; Heredia, C.; Tessier, E.; Gassie, C.; Point, D.; Guédron, S.; et al. Linking microbial activities and low molecular weight thiols to Hg methylation in biofilms and periphyton from high altitude tropical lakes (Bolivian altiplano). *Environ. Sci. Technol.* **2018**, *52*, 9758–9767. [CrossRef] [PubMed]

16. Guédron, S.; Devin, S.; Vignati, D.A.L. Total and methylmercury partitioning between colloids and true solution: From case studies in sediment overlying and porewaters to a generalized model. *Environ. Toxicol. Chem.* **2016**, *35*, 330–339. [CrossRef] [PubMed]
17. Helbling, E.W.; Villafañe, V.; Buma, A.; Andrade, M.; Zaratti, F. DNA damage and photosynthetic inhibition induced by solar ultraviolet radiation in tropical phytoplankton (Lake Titicaca, Bolivia). *Eur. J. Phycol.* **2001**, *36*, 157–166. [CrossRef]
18. Alanoca, L.; Amouroux, D.; Monperrus, M.; Tessier, E.; Goni, M.; Guyoneaud, R.; Achá, D.; Gassie, C.; Audry, S.; Garcia, M.; et al. Diurnal variability and biogeochemical reactivity of mercury species in an extreme high altitude lake ecosystem of the Bolivian Altiplano. *Environ. Sci. Pollut. Res.* **2016**, *23*, 6919–6933. [CrossRef]
19. Alanoca, L.; Guédron, S.; Amouroux, D.; Audry, S.; Monperrus, M.; Tessier, M.; Goix, S.; Achá, D.; Seyler, P.; Point, D. Synergistic effects of mining and urban effluents on the level and distribution of methylmercury in a shallow aquatic ecosystem of the Bolivian Altiplano. *Environ. Sci. Process. Impacts* **2016**, *18*, 1550–1560. [CrossRef]
20. Tapia, J.; Audry, S.; van Beek, P. Natural and anthropogenic controls on particulate metal(loid) deposition in Bolivian highland sediments, Lake Uru Uru (Bolivia). *Holocene* **2020**, *30*, 428–440. [CrossRef]
21. Sarret, G.; Guédron, S.; Achá, D.; Bureau, S.; Arnaud-Godet, F.; Tisserand, D.; Goni-Urriza, M.; Gassie, C.; Duwig, C.l.; Proux, O.; et al. Extreme Arsenic Bioaccumulation Factor Variability in Lake Titicaca, Bolivia. *Sci. Rep.* **2019**, *9*, 10626. [CrossRef]
22. Tapia, J.; Audry, S. Control of early diagenesis processes on trace metal (Cu, Zn, Cd, Pb and U) and metalloid (As, Sb) behaviors in mining-and smelting-impacted lacustrine environments of the Bolivian Altiplano. *Appl. Geochem.* **2013**, *31*, 60–78. [CrossRef]
23. Guédron, S.; Grimaldi, M.; Grimaldi, C.; Cossa, D.; Tisserand, D.; Charlet, L. Amazonian former gold mined soils as a source of methylmercury: Evidence from a small scale watershed in French Guiana. *Wat. Res.* **2011**, *45*, 2659–2669. [CrossRef]
24. Guédron, S.; Point, D.; Achá, D.; Bouchet, S.; Baya, P.A.; Molina, C.I.; Tessier, E.; Monperrus, M.; Flores, M.; Fernandez Saavedra, P.; et al. Mercury contamination level and speciation inventory in the hydrosystem of Lake Titicaca: Current status and future trends. *Environ. Pollut.* **2017**, *231*, 262–270. [CrossRef] [PubMed]
25. Bloom, N.S.; Fitzgerald, W.F. Determination of volatile mercury species at the picogram level by low-temperature gas chromatography with cold-vapor atomic fluorescence detection. *Anal. Chim. Acta* **1988**, *208*, 151–161. [CrossRef]
26. Cossa, D.; Averty, B.; Pirrone, N. The origin of methylmercury in open Mediterranean waters. *Limnol. Oceanogr.* **2009**, *54*, 837–844. [CrossRef]
27. Guédron, S.; Duwig, C.; Prado, B.L.; Point, D.; Flores, M.G.; Siebe, C. (Methyl) Mercury, Arsenic, and Lead Contamination of the World's Largest Wastewater Irrigation System: The Mezquital Valley (Hidalgo State-Mexico). *Water Air Soil Pollut.* **2014**, *225*, 1–19. [CrossRef]
28. Achá, D.; Guédron, S.; Amouroux, D.; Point, D.; Lazarro, X.; Fernandez, P.; Sarret, G. Algal bloom exacerbates hydrogen sulfide and methylmercury contamination in the emblematic high-altitude Lake Titicaca. *Geosciences* **2018**, *8*, 438. [CrossRef]
29. Monperrus, M.; Gonzalez, P.R.; Amouroux, D.; Alonso, J.I.G.; Donard, O.F.X. Evaluating the potential and limitations of double-spiking species-specific isotope dilution analysis for the accurate quantification of mercury species in different environmental matrices. *Anal. Bioanal. Chem.* **2008**, *390*, 655–666. [CrossRef]
30. Sharif, A.; Monperrus, M.; Tessier, E.; Bouchet, S.; Pinaly, H.; Rodriguez-Gonzalez, P.; Maron, P.; Amouroux, D. Fate of mercury species in the coastal plume of the Adour River estuary (Bay of Biscay, SW France). *Sci. Total Environ.* **2014**, *496*, 701–713. [CrossRef]
31. Small, J.M.; Hintelmann, H. Methylene blue derivatization then LC-MS analysis for measurement of trace levels of sulfide in aquatic samples. *Anal. Bioanal. Chem.* **2007**, *387*, 2881–2886. [CrossRef]
32. Small, J.M.; Hintelmann, H. Sulfide and mercury species profiles in two Ontario boreal shield lakes. *Chemosphere* **2014**, *111*, 96–102. [CrossRef] [PubMed]
33. Berner, R.A. *Early Diagenesis*; Princeton University Press: Princeton, NJ, USA, 1980; p. 240.
34. Boudreau, B.P. The diffusive tortuosity of fine-grained unlithified sediments. *Geochim. Cosmochim. Acta* **1996**, *60*, 3139–3142. [CrossRef]

35. Rothenberg, S.E.; Ambrose, R.F.; Jay, J.A. Mercury cycling in surface water, pore water and sediments of Mugu Lagoon, CA, USA. *Environ. Pollut.* **2008**, *154*, 32–45. [CrossRef]
36. Dill, C.; Kuiken, T.; Zhang, H.; Ensor, M. Diurnal variation of dissolved gaseous mercury (DGM) levels in a southern reservoir lake (Tennessee, USA) in relation to solar radiation. *Sci. Total Environ.* **2006**, *357*, 176–193. [CrossRef]
37. Amyot, M.; Mierle, G.; Lean, D.; McQueen, D.J. Effect of solar radiation on the formation of dissolved gaseus mercury in temperate lakes. *Geochim. Cosmochim. Acta* **1997**, *61*, 975–987. [CrossRef]
38. Soerensen, A.L.; Schartup, A.T.; Gustafsson, E.; Gustafsson, B.G.; Undeman, E.; Björn, E. Eutrophication Increases Phytoplankton Methylmercury Concentrations in a Coastal Sea -¸ A Baltic Sea Case Study. *Environ. Sci. Technol.* **2016**, *50*, 11787–11796. [CrossRef]
39. Lei, P.; Nunes, L.M.; Liu, Y.-R.; Zhong, H.; Pan, K. Mechanisms of algal biomass input enhanced microbial Hg methylation in lake sediments. *Environ. Int.* **2019**, *126*, 279–288. [CrossRef]
40. Knorr, K.H. DOC-dynamics in a small headwater catchment as driven by redox fluctuations and hydrological flow paths—Are DOC exports mediated by iron reduction/oxidation cycles? *Biogeosciences* **2013**, *10*, 891–904. [CrossRef]
41. Feyte, S.P.; Gobeil, C.; Tessier, A.; Cossa, D. Mercury dynamics in lake sediments. *Geochim. Cosmochim. Acta* **2012**, *82*, 92–112. [CrossRef]
42. Hellal, J.; Guédron, S.; Huguet, L.; Schaefer, J.; Laperche, V.; Joulian, C.; Lanceleur, L.; Burnol, A.; Ghestem, J.-P.; Garrido, F.; et al. Mercury mobilization and speciation linked to bacterial iron oxide and sulfate reduction: A column study to mimic reactive transfer in an anoxic aquifer. *J. Contam. Hydrol.* **2015**, *180*, 56–68. [CrossRef]
43. Benoit, J.M.; Gilmour, C.C.; Mason, R.P. Aspects of bioavailability of mercury for methylation in pure cultures of *Desulfobulbus propionicus* (1pr3). *Appl. Environ. Microbiol.* **2001**, *67*, 51–58. [CrossRef]
44. Gill, G.A.; Bloom, N.S.; Cappellino, S.; Driscoll, C.T.; Dobbs, C.; McShea, L.; Mason, R.; Rudd, J.W.M. Sediment-water fluxes of mercury in Lavaca Bay, Texas. *Environ. Sci. Technol.* **1999**, *33*, 663–669. [CrossRef]
45. Pickhardt, P.C.; Fisher, N.S. Accumulation of Inorganic and Methylmercury by Freshwater Phytoplankton in Two Contrasting Water Bodies. *Environ. Sci. Technol.* **2007**, *41*, 125–131. [CrossRef]
46. Quiroga-Flores, R.; Guédron, S.; Achá, D. High methylmercury uptake by green algae in Lake Titicaca: Potential implications for remediation. *Ecotoxicol. Environ. Saf.* **2020**, *207*, 111256. [CrossRef]
47. Point, D.; Bareille, G.; Pinaly, H.; Belin, C.; Donard, O.F.X. Multielemental speciation of trace elements in estuarine waters with automated on-site UV photolysis and resin chelation coupled to inductively coupled plasma mass spectrometry. *Talanta* **2007**, *72*, 1207–1216. [CrossRef] [PubMed]
48. Achá, D.; Pabon, C.A.; Hintelmann, H. Mercury methylation and hydrogen sulfide production among unexpected strains isolated from periphyton of two macrophytes of the Amazon. *FEMS Microbiol. Ecol.* **2012**, *80*, 637–645. [CrossRef]
49. Gascon Diez, E.; Loizeau, J.-L.; Cosio, C.; Bouchet, S.; Adatte, T.; Amouroux, D.; Bravo, A.G. Role of settling particles on mercury methylation in the oxic water column of freshwater systems. *Environ. Sci. Technol.* **2016**, *50*, 11672–11679. [CrossRef]
50. Audry, S.; Blanc, G.; Schäfer, J.; Chaillou, G.N.L.; Robert, S.B. Early diagenesis of trace metals (Cd, Cu, Co, Ni, U, Mo, and V) in the freshwater reaches of a macrotidal estuary. *Geochim. Cosmochim. Acta* **2006**, *70*, 2264–2282. [CrossRef]
51. Wanty, R.B.; Goldhaber, M.B. Thermodynamics and kinetics of reactions involving vanadium in natural systems: Accumulation of vanadium in sedimentary rocks. *Geochim. Cosmochim. Acta* **1992**, *56*, 1471–1483. [CrossRef]
52. Graham, A.M.; Cameron-Burr, K.T.; Hajic, H.A.; Lee, C.; Msekela, D.; Gilmour, C.C. Sulfurization of Dissolved Organic Matter Increases Hg-Sulfide-Dissolved Organic Matter Bioavailability to a Hg-Methylating Bacterium. *Environ. Sci. Technol.* **2017**, *51*, 9080–9088. [CrossRef]
53. Von Wachenfeldt, E.; Tranvik, L.J. Sedimentation in Boreal Lakes: The Role of Flocculation of Allochthonous Dissolved Organic Matter in the Water Column. *Ecosystems* **2008**, *11*, 803–814. [CrossRef]
54. Yan, J.; Lazouskaya, V.; Jin, Y. Soil colloid release affected by dissolved organic matter and redox conditions. *Vadose Zone J.* **2016**, *15*, 1–10. [CrossRef]
55. Lanza, W.G.; Achá, D.; Point, D.; Masbou, J.; Alanoca, L.; Amouroux, D.; Lazzaro, X. Association of a Specific Algal Group with Methylmercury Accumulation in Periphyton of a Tropical High-Altitude Andean Lake. *Arch. Environ. Contam. Toxicol.* **2017**, *72*, 1–10. [CrossRef]

56. Moye, H.A.; Miles, C.J.; Phlips, E.J.; Sargent, B.; Merritt, K.K. Kinetics and Uptake Mechanisms for Monomethylmercury between Freshwater Algae and Water. *Environ. Sci. Technol.* **2002**, *36*, 3550–3555. [CrossRef]
57. Deng, L.; Fu, D.; Deng, N. Photo-induced transformations of mercury(II) species in the presence of algae, Chlorella vulgaris. *J. Hazard. Mater.* **2009**, *164*, 798–805. [CrossRef]
58. Andrade, M.; Forno, R.; Palenque, E.; Zaratti, F. Estudio preliminar del efecto de altura sobre la radiación solar ultravioleta B. *Rev. Bol. Fis.* **1998**, *4*, 14.
59. Blumthaler, M.; Ambach, W.; Rehwald, W. Solar UV-A and UV-B radiation fluxes at two alpine stations at different altitudes. *Theor. Appl. Climatol.* **1992**, *46*, 39–44. [CrossRef]
60. Villafae, V.E.; Andrade, M.; Lairana, V.; Zaratti, F.; Helbling, E.W. Inhibition of phytoplankton photosynthesis by solar ultraviolet radiation: Studies in Lake Titicaca, Bolivia. *Freshw. Biol.* **1999**, *42*, 215–224. [CrossRef]
61. Klapstein, S.J.; O'Driscoll, N.J. Methylmercury biogeochemistry in freshwater ecosystems: A review focusing on DOM and photodemethylation. *Bull. Environ. Contam. Toxicol.* **2018**, *100*, 14–25. [CrossRef]
62. Oremland, R.S.; Culbertson, C.W.; Winfrey, M.R. Methylmercury decomposition in sediments and bacterial cultures: Involvement of methanogens and sulfate reducers in oxidative demethylation. *Appl. Environ. Microbiol.* **1991**, *57*, 130–137. [CrossRef] [PubMed]
63. Klapstein, S.J.; Ziegler, S.E.; O'Driscoll, N.J. Methylmercury photodemethylation is inhibited in lakes with high dissolved organic matter. *Environ. Pollut.* **2018**, *232*, 392–401. [CrossRef] [PubMed]
64. Klapstein, S.J.; Ziegler, S.E.; Risk, D.A.; O'Driscoll, N.J. Quantifying the effects of photoreactive dissolved organic matter on methylmercury photodemethylation rates in freshwaters. *Environ. Toxicol. Chem.* **2017**, *36*, 1493–1502. [CrossRef]
65. Jeremiason, J.D.; Portner, J.C.; Aiken, G.R.; Hiranaka, A.J.; Dvorak, M.T.; Tran, K.T.; Latch, D.E. Photoreduction of Hg (II) and photodemethylation of methylmercury: The key role of thiol sites on dissolved organic matter. *Environ. Sci. Process. Impacts* **2015**, *17*, 1892–1903. [CrossRef] [PubMed]
66. Ni, B.; Kramer, J.R.; Bell, R.A.; Werstiuk, N.H. Protonolysis of the Hgâˆ' C Bond of chloromethylmercury and dimethylmercury. A DFT and QTAIM Study. *J. Phys. Chem. A* **2006**, *110*, 9451–9458. [CrossRef] [PubMed]
67. Zhang, D.; Yin, Y.; Li, Y.; Cai, Y.; Liu, J. Critical role of natural organic matter in photodegradation of methylmercury in water: Molecular weight and interactive effects with other environmental factors. *Sci. Total Environ.* **2017**, *578*, 535–541. [CrossRef] [PubMed]
68. SENAMHI, B. Servicio Nacional de Meteorología de Hidrología. *La PazBoliv*. Available online: http://www.senamhi.gob.bo (accessed on 25 August 2020).